Malaysian Journal of Catalysis 3 (2018) 29-31

Malaysian Journal of Catalysis

http://mjcat.utm.my/

MJCat

Enhancing the performance of dye-sensitized solar cells by incorporating various ratios of platinum and reduced graphene oxide thin film as a counter electrode

A. Bolhana, N. A. Ludina*, , M. S. Suaita, M. A. Mat-Teridia, K. Sopiana, Norani Muti Mohamedb, H. Arakawac
[a]Solar Energy Research Institute (SERI), Universiti Kebangsaan Malaysia, 43600 Bangi, Selangor, MALAYSIA, [b]Centre of Innovative Nanostructures & Nanodevices (COINN), University Teknologi PETRONAS (UTP), 32610 Seri Iskandar, Perak Darul Ridzuan, MALAYSIA, [c]Department of Industrial Chemistry, Faculty of Engineering, Tokyo University of Science, 162-0826, JAPAN
*Corresponding author email: sheekeen@ukm.edu.my

Article history :
Received 1 September 2016
Accepted 24 August 2017

GRAPICAL ABSTRACT

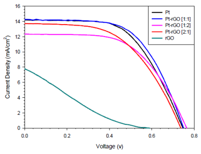

ABSTRACT

A platinum/reduced graphene oxide (Pt-rGO) thin film was prepared and deposited on a fluorine-doped tin oxide (FTO) substrate using the doctor blade method and was annealed at 450 °C for 30 minutes. Thin films were used as counter electrode in a dye-sensitized solar cell (DSSC) with Pt-rGO ratios of 1:1, 1:2, and 2:1. Cyclic voltammetry showed that the Pt-rGO thin film with a ratio of 1:1 exhibits better electrocatalytic activity for I_3^-/I^- redox reaction. The current-voltage curve (I-V) revealed that DSSC using the Pt-rGO CE thin film with a ratio of 1:1 has a power conversion efficiency (PCE) of 6.3% under AM 1.5 illumination of 100 mW cm^{-2} and this is higher than Pt (6.1%). The current density (Jsc) is 14.3 mA/cm^{-2}, open circuit voltage (Voc) is 0.75 V, and fill factor (FF) is 58.98.

Keywords: reduced graphene oxide, platinum, counter electrode, dye-sensitized solar cell)

© 2018 Dept. of Chemistry, UTM. All rights reserved. || eISSN 0128-2581 ||

1. INTRODUCTION

Since the pioneering of the dye-sensitized solar cell with power energy conversion of 7.1% discovered by Gratzel and O'Regan in 1991 [1,2], the dye-sensitized solar cell (DSSC) has attracted considerable interest because of the low cost and simplicity of its fabrication process and its high power conversion efficiency [1–6]. The DSSC structure consists of a dye-sensitized TiO2 photoanode electrode, an electrolyte, and a platinum (Pt) counter electrode (CE) [1–6]. Pt is the most suitable material for CE because of its outstanding electrocatalytic activity toward I3- reduction, fast electron transfer at CE/electrolyte interface, and high conductivity [6]. However, Pt is expensive, limiting the application of the DSSC [6, 7]. Therefore, an alternative low cost material to replace Pt is needed to enhance the commercialization potential of DSSC. One of the alternative materials that are the subject of intense investigation is carbon based materials [5–7]. Carbon materials include carbon black, activated carbon, graphite, carbon nanotubes, and graphene [5–7]. Among these carbon materials, graphene is the most promising as CE material because of its large surface area, low cost, corrosion resistance, and good electrical conductivity [5–7]. Graphene is a 2D sheet of covalent bonded carbon atoms with good catalytic activity and intrinsic long range of π-π electronic structure, which contributes to its excellent electronic mobility [8-10]. Numerous research teams have used graphene as material for the CE. Yue et al. (2013) prepared Pt/graphene nanosheet (GN) by the electrodeposition method using three electrode cell systems. Among the various weight ratios of Pt/GN, the GN with a ratio of 0.15 wt.% gained the highest efficiency of 7.88%. Tsai et al. (2015) fabricated GN-Pt using GN-Pt composite and GN-Pt stacked. GN-Pt stacked was reported to have a high efficiency of 8.54%. Duan et al. (2013) prepared graphene using the modified Hummer's method and determined that graphene provides a large surface area that helps in the diffusion of electrolytes in CE increasing catalytic activity.

The present paper reports the performance of DSSC with various ratios of Pt and reduced graphene oxide as a counter electrode deposited on fluorine-doped tin oxide (FTO) using the doctor blade method. Electrochemical properties, such as cyclic voltammetry is measured and studied. The counter electrode is characterized using X-ray diffraction (XRD) to investigate the crystallite size of the thin film. The *IV* performance of the DSSC incorporating these materials is also investigated

2. MATERIALS AND METHODS

2.1 Materials

Graphene oxide synthesized using graphite nanopowder by modified hummer method was purchased from US Research Nanomaterials and platinum paste PT-1 purchased from Dyesol-Australia were use as counter electrode materials. TiO2 WER2-0 as photoanode material, N719 as Ruthenium dye sensitizer, 8 Ω cm^{-2} FTO glass substrate (FTO Tec 8) and 15 Ω cm^{-2} FTO glass substrate (FTO Tec 15) also purchased from Dyesol-Australia. Iodide electrolyte (Iodolyte, AN-50) purchased from solaronix-Switzerland performed as electrolyte.

2.2 Methodology

Graphene oxide (GO) was prepared using the modified hummer method [9]. GO was sonicated with distilled water in a beaker for about 5 hours to produce homogeneous mixture. The mixture with a concentration of 0.3 mg/cm-3 was poured into a jar with graphite sheet and left to evaporate overnight in an oven at 60 °C. The graphene oxide paste was then mixed with commercial Pt paste at weight ratios (Pt:GO) of 2:1, 1:1 and 1:2. The mixed paste was then deposited onto a 1.5 cm x 2 cm, 8 Ω cm^{-2} FTO glass substrate using the doctor blade method and was post treated by annealling for about 30 minutes at 450 °C. The GO was reduced to rGO after the post treatment. The Pt and rGO thin film were prepared using similar procedure. TiO_2 photoanode thin films were deposited onto a 2.5 cm x 2 cm, 15 Ω cm^{-2} FTO thin film with an active area of 0.25 cm^2 using the doctor blade method annealed at 450 °C for 30 minutes. The photoanode was then immersed in the solution mixture of 0.3 mM ethanol and N719 for about 16 hours. The cell was assembled in sandwich arrangement with Surlyn to attach the photoanode and counter electrode together. The fabrication of the DSSC cell was completed by injecting the liquid iodide electrolyte in the aperture between the photoanode electrode and CE.

2.2 Characterizations

The CE thin film potential and complete DSSC cell performance were analyzed using several characterizations. XRD (D8 advanced, Bruker) analysis was used to determine the crystallite size of the inorganic component, whereas the electrocatalytic activity of the CE thin film was analyzed using cyclic voltammetry (CV) (Autolab PGSTAT). The photovoltaic performance was examined by current-voltage (*IV* characteristic) (LIV tester software and AAA simulator).

3. RESULTS AND DISCUSSION

3.1 X-ray Diffraction Analyses

Fig. 1 shows the XRD pattern of Pt, Pt-rGO (1:1), Pt-rGO (1:2), Pt-rGO (2:1), and rGO CE thin films annealed at 450°C. Pt has a prominent peak observed at (111) plane (JCPDS 01-070-2431). The Pt peak decreases when the ratio of rGO increases. The diffraction of rGO is 26.68° traced as *hkl* plane (005) (JCPDS 00-026-1077). Pt CE thin film XRD pattern shows diffraction at 26.58°, similar to the diffraction of rGO. However, this diffraction belongs to tin oxide (SnO2) with JSPDS of 01-077-3163, in which the diffraction angle is near the rGO. Almost no diffraction of rGO is visible at Pt-rGO (2:1) CE thin film XRD pattern because the intensity of rGO is weaker than that of Pt, which displays the highest peak of diffraction.

The crystallite of the CE thin film can be calculated using the following Debye–Scherrer equatian [10],

$$D = \frac{0.9\lambda}{\beta\cos\theta}$$

where D is the crystallite size; λ is the wavelength of the incident X-rays; β is the full width at half maximum in radians; and, θ is the diffraction angle. The crystallite sizes of Pt, Pt-rGO (1:1), Pt-rGO (1:2), Pt-rGO (2:1), and rGO CE thin films are organized in Table 1. Pt is a smaller crystallite than rGO; thus, the addition of rGO to the Pt particle increases the crystallite size of the Pt-rGO composite.

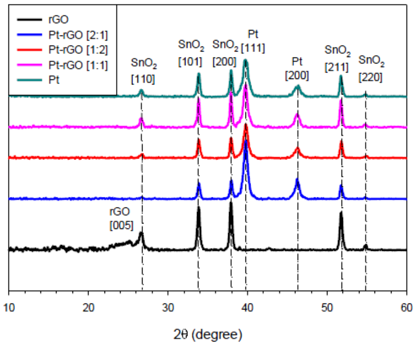

Fig. 1 X-ray diffraction patterns of the counter electrode thin film

Table 1 Crystallite sizes of Pt, Pt-rGO (1:1), Pt-rGO (1:2), Pt-rGO (2:1), and rGO thin films

Thin Film	Pt	Pt-rGO [1:1]	Pt-rGO [1:2]	Pt-rGO [2:1]	rGO
Crystallite Size	32.014	64.714	74.714	36.115	55.900

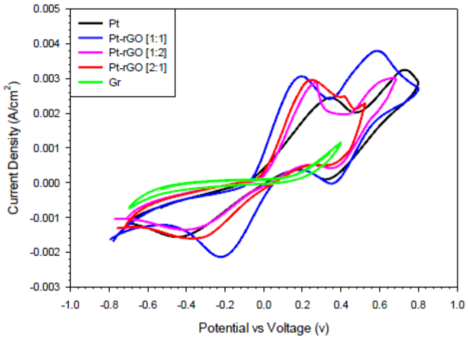

Fig. 2 CV of the CE thin film Pt, Pt-rGO [1:1], Pt-rGO [1:2], Pt-rGO [2:1], and rGO

3.2 Cyclic Voltammetry (CV) analysis

The condition of the redox reaction of iodide ion has an important role in the work function at the CE of DSSC [11]. The CE thin film was investigated through CV analysis, and an electrolyte solution containing iodide/triiodide was used in the measurement. Fig. 2 shows the CV for Pt, Pt-rGO [1:1], Pt-rGO [1:2], Pt-rGO [2:1], and rGO at a scan rate of 10 mVs^{-1}, in which two pair of oxidation and reduction peaks can be observed. Peaks I and I1 represent oxidation of anodic current meanwhile II and II1 represent reduction of cathodic current [11]. The peak II represents the reduction reaction I_3^- +2e$^-$ $\longrightarrow$3I$^-$, which occurs at the CE of DSSC [10]. Meanwhile, the peak I represents the oxidation reaction 3I-$\longrightarrow$ I_3^-+2e$^-$. However, this peak is unimportant in the DSSC [11]. Noticeably the Pt-rGO [1:1] CE shows a higher reduction of cathodic current -2.11 mA/cm^{-2} at -0.227 V.

3.3 Current Voltage Characteristics

Fig. 3 shows the IV curves of the DSSC-based Pt, Pt-rGO [1:1], Pt-rGO [1:2], Pt-rGO [2:1], and rGO thin films CE. The energy conversion efficiency of the solar cell is calculated by [12]

$$\eta = \frac{VocJscFF}{Pin}$$

where Pin is the optical power of 100 mWcm^{-2} under AM 1.5. Table 2 summarizes the photovoltaic parameters. The Jsc, Voc, *FF*, and efficiency of Pt are 14.4 mA/cm^{-2}, 0.747 V, 57.08, and 6.1%, respectively. The CE of Pt-rGO [1:1] enhances the efficiency up to 6.3% with Jsc, Voc, and FF of 14.3 mA/cm^{-2}, 0.75 V, and 58.98, respectively. The enhanced efficiency is due to the high catalytic activity for I_3^- reduction, as proven in the CV measurement. The rGO CE has the lowest efficiency, as well as Jsc, which is attributed to the low catalytic activity but high electrolyte diffusion [8].

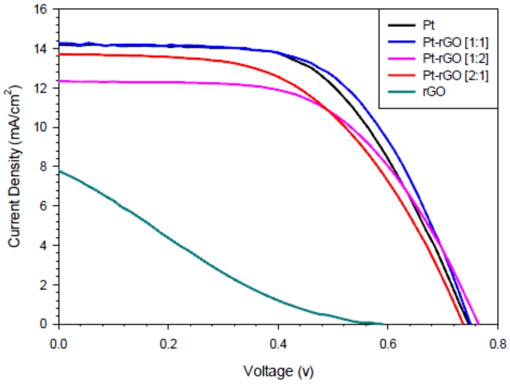

Fig. 3 IV curve of the CE thin film: Pt, Pt-rGO [1:1], Pt-rGO [1:2], Pt-rGO [2:1], and rGO

DSSC-based Pt-rGO [1:1] as a CE has the highest efficiency value of 6.3% because a low value of Rct (19.42 Ω) indicates high catalytic activity in CE, thereby possibly enhancing the value of Jsc (14.3 mA/cm^2) and contributing to a higher value of *FF* (58.98). The DSSC with Pt CE and rGO CE have similar Jsc and Voc but latter has higher FF, thereby yielding slightly higher efficiency than the DSSC with Pt CE. This [1:1] ratio of Pt-rGO CE based on weight can be further studied to optimize the DSSC performance.

Table 2 Photovoltaic parameter of DSSC

Thin film	V_{oc} (V)	J_{sc} (mA/cm^2)	*FF*	R_s (Ω)	R_{ct} (Ω)	R_s (Ω)	R_{ct} (Ω)	Efficiency, η (%)
				Counter electrode		Full DSSC device		
Pt	0.747	14.2	57.08	29711	81408	12.665	10.451	6.1
Pt-rGO [1:1]	0.75	14.3	58.98	-4155.8	1.10E+05	12.972	19.42	6.3
Pt-rGO [1:2]	0.765	12.3	56.72	22591	-18283	54.869	95.464	5.4
Pt-rGO [2:1]	0.737	13.7	52.85	25957	2.78E+05	32.466	78.912	5.3
rGO	0.592	7.8	19.22	42.063	51.229	17.217	585.1	0.9

4. CONCLUSION

Please The Pt-rGO CE of various ratios was successfully prepared and deposited on an FTO glass substrate by the doctor blade method and annealed at 450 °C for 30 minutes. The Pt-rGO counter electrode thin film with a ratio of [1:1] has higher catalytic activity as proven by the CV measurement. In the CV measurement the high catalytic activity is illustrated by the highest reduction reaction I_3^-+2e$^-$ $\rightarrow$3I$^-$ (-2.11 mA/cm^{-2} at -0.227 V). The reduction process is the crucial process at the CE of DSSC because of its role in improving cell performance. As the result, the DSSC fabricated with Pt-rGO [1:1] counter electrode has a value of Rct of 19.42 Ω and a higher value of Jsc (14.3 mA/cm^{-2}), FF (58.98), and η of 6.3%, as presented in Table 2.

REFERENCES

[1] M. Gratzel, B. O'Regan, *Nature* 353 (1971) 737.
[2] J. Gong, J. Liang, K. Sumathy, *Renew. Sustainable Energy Rev*.16 (2012) 5484-5860.
[3] M. Gratzel, *Nature* 414 (2001) 338.
[4] A. Yella, H. Lee, H. Tsao, C. Yi, A.K. Chandiran, M.K Nazeeruddin, E.W.G. Diau, C.Y. Yeh, S.M Zakeeruddin, M. Gratzel, *Science* 334 (2011) 629.
[5] G. Yue, J. Wu, Y. Xiao, M. Huang, J. lin, L. Fan, Z. Lan, *Electrochim. Acta* 92 (2013) 64.
[6] L. Qiu, H. Zhang, W. Wang, Y. Chen, R. Wang, *Appl. Surf. Sci.* 319 (2014) 339.
[7] C.-Y. Liu, K.-C Huang, P.-H. Chung, C.-C. Wang, C.-Y. Chen, R. Vittal, C.-G. Wu, W.-Y. Chiu, K.-C. Ho, *J. Power Sources* 217 (2012) 152.
[8] X. Duan, Z. Gao, J. Chang, D. Wu, P. Ma, J. He, F. Xu, S. Gao, K. Jiang, *Electrochim. Acta*114 (2013) 173.
[9] W. J. Basirun, M. Sookhakian, S. Baradaran, Z. Endut, M. R. Mahmoudian, M. Ebadi, R. Yousefi, H. Ghadimi, S. Ahmed, *Sci. Rep.* 5 (2015) 9108.
[10] H. Lipson, H. Steeple, *Macmillan, London,* 1970.
[11] S.-H. Chang, M.-D. Lu, Y.-L. Tung, H.-Y. Tuan, *ASC nano* 7 (2013) 9443.
[12] A. B. F. Martinson, M. S. Goes, F. Fabregat-Santiago, J. Bisquert, M. J. Pellin, J. T. Hupp, *J. Phys. Chem. A.*, 113 (2009) 4015.